Climate Resilience through AI-Driven Hurricane Damage Assessments

Deepank Kumar Singh, Vedhus Hoskere
University of Houston
dksingh@uh.edu, vhoskere@uh.edu

Abstract

Evolving hurricane patterns intensified by climate change are expected to exacerbate economic hardships on coastal communities. Climate resilience for these communities requires both the capability to recover rapidly from devastating storms, and the ability to develop an accurate and actionable understanding of vulnerabilities to reduce the impact of future storms. Available data from past storms can provide invaluable insight in addressing both these requirements. Post-disaster preliminary damage assessments (PDAs) are a crucial initial step toward a rapid recovery. They also provide the most accurate information on the performance of various types of dwellings after the storm. Traditional door-to-door inspection methods are time-consuming and can hinder efficient resource allocation by governments in the aftermath. To address this, researchers have proposed automated PDA frameworks, often utilizing data from satellites, combined with deep convolutional neural networks. However, before such frameworks can be adopted in practice, the accuracy and fidelity of predictions of damage level at the scale of an entire building must be comparable to human assessments. To bridge this gap, we present an innovative PDA framework that leverages Ultra-High-Resolution Aerial (UHRA) images alongside state-of-the-art transformer models for multi-class damage predictions across entire buildings. Our approach leverages vast amounts of unlabeled data to enhance accuracy of prediction and generalization capabilities. Through a series of experiments, we evaluate the influence of incorporating unlabeled data, and transformer models. By integrating UHRA images and semi-supervised transformer models, our findings indicate that this framework overcomes critical limitations associated with satellite imagery and traditional CNN models, achieving an 88% multiclass accuracy, ultimately leading to more precise, efficient, and reliable damage assessments that are a first step towards building more climate resilient societies.

Introduction

As a result of climate change, warmer sea surface temperatures are driving the intensification of tropical storm wind speeds, amplifying their potential for damage upon making landfall. Over the 39-year period from 1979 to 2017, a noteworthy shift has been observed, with an increase in the frequency of major hurricanes and a decrease in the number of smaller hurricanes. Looking ahead, predictive modeling by the National Oceanic and Atmospheric Administration points to a future marked by heightened occurrences of Category 4 and 5 hurricanes, accompanied by elevated hurricane wind speeds (Irish et al., 2014; Woodward & Samet, 2018). In the process of recovery, the initial crucial step following a hurricane is conducting Preliminary Damage Assessments (PDAs). Preliminary Damage Assessments (PDA) evaluate the extent of damage caused by disasters to buildings and are the first step in the post-disaster recovery process. These damage assessments are necessary after disasters to ensure the safety of buildings and allocate government resources to homeowners. Due to Climate change, the increasing number of category 4 and 5 hurricanes could potentially result in hundreds of thousands of IA applications (Reese 2018), overwhelming the available workforce and rendering the number of inspectors and support staff inadequate to meet the demands of comprehensive evaluations. There is thus a need for alternative methods that can help accelerate the PDA process.

Various data sources have been explored for their applicability in post-disaster damage assessments, satellites (optical and SAR) (Celik, 2009, 2010; Chen et al., 2021; Gupta, Goodman, et al., 2019; Kim et al., 2023; Lu et al., 2018; Matsuoka & Yamazaki, 2004, 2005; Watanabe et al., 2016), unmanned aerial vehicles (UAVs) (Ezequiel et al. 2014; Aicardi et al. 2016; Mavroulis et al. 2019; Calantropio et al. 2021; Rahnemoonfar et al. 2022), and ground-level cameras (Hoskere et al. 2018; Narazaki et al. 2022; Khajwal et al. 2023). Satellite images are commonly used due to their wide availability, as seen in datasets like xBD which provides pre- and post-event satellite imagery with annotated building damage levels. However, satellite

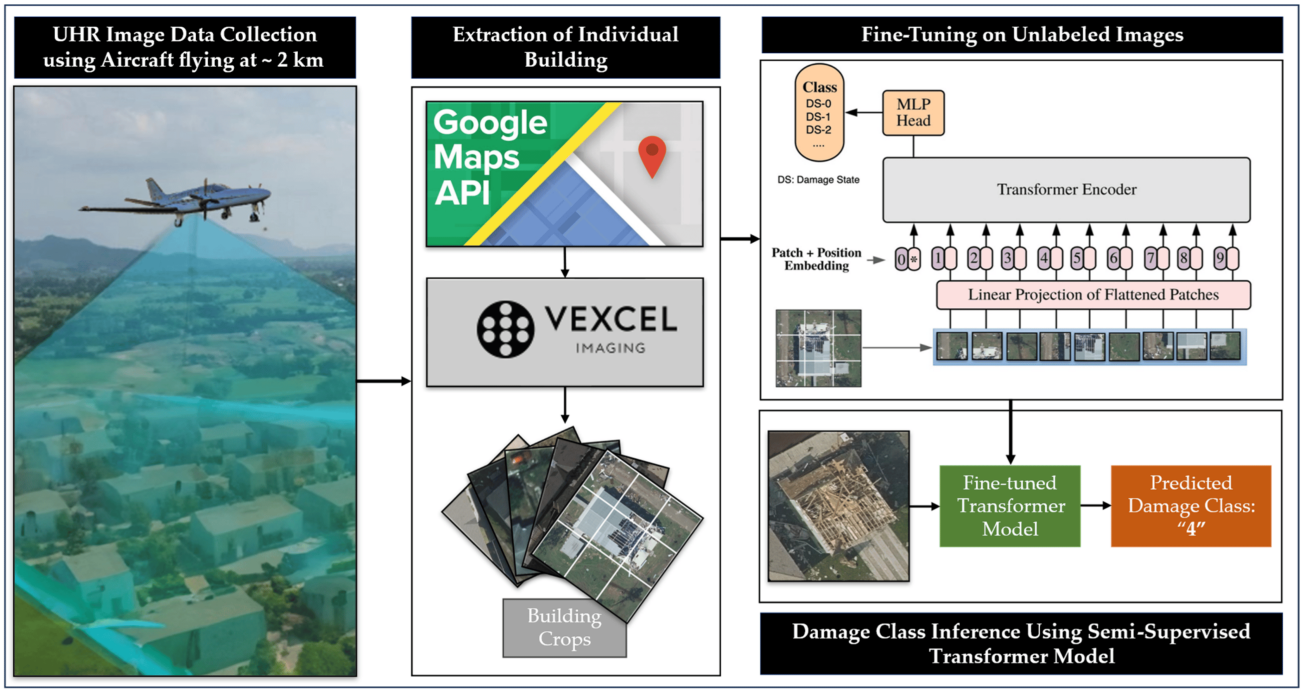

Figure 1. Proposed PDA Framework

imagery can be hindered by overcast conditions and limited resolution affecting accuracy. Researchers have proposed methods utilizing both pre- and post-disaster satellite imagery, though pre-disaster data may not always be available (Singh and Hoskere 2023). Synthetic Aperture Radar (SAR) images offer alternatives to optical satellite images, compensating for cloud occlusions but may face challenges in assessing individual buildings due to low resolution. UAV data offers high-resolution images, yet is constrained by flight time, coverage area, and weather conditions. Ground-level camera images provide close-up perspectives but struggle with scalability and accessibility issues. Each data type carries limitations, underscoring the need for thoughtful selection when enhancing post-disaster assessments.

Post-processing methods, along with data sources, significantly influence assessment accuracy. Researchers have delved into heuristic and deep learning techniques for tasks like damage classification and change detection. Analysis often centers on bitemporal satellite images, capturing pre- and post-disaster states, enabling visible differences. Approaches encompass pixel-to-pixel comparisons (Celik 2010; Asokan and Anitha 2019) and deep learning (Bai et al. 2020; Lee et al. 2020; Abdi and Jabari 2021; Calantropio et al. 2021; Rahnemoonfar et al. 2022). For instance, during Hurricane Michael, (Berezina and Liu 2022) employed a U-Net model for segmentation and a ResNet CNN architecture for classification, highlighting the superiority of deep neural networks over traditional classifiers. Similarly, introduced EBDC-Net (Hong Zhong 2022) to refine damaged building classification after earthquakes. Change detection studies usually involve limited damage classes, often binary. A recent study by Khajwal et al. (Khajwal et al. 2023) achieved an initial 55% accuracy using a single satellite image and an additional 10% boost through multi-view ground images.

We present a new PDA framework (Figure 1) that combines Ultra-High-Resolution Aerial (UHRA) imagery and semi-supervised learning to enhance multi-class damage classification accuracy. Our study explores diverse data types, contrasting our approach with current methods.

Proposed Methods

Our framework for PDA is illustrated in Figure 1. The process consists of four steps. Firstly, raw UHRA image data is collected by using an aircraft equipped with an ultra-high-resolution image sensor, (e.g., UltraCam from Vexcel Imaging), typically within 2-3 days after a hurricane strikes. For instance, after Hurricane Michael, the data for an 85,000 sq-km area across four states was published online in just over three days[1].Then, the collected data is processed to

[1] https://www.vexcel-imaging.com

Figure 2. Samples for UHRA and satellite images with corresponding damage class.

extract individual building crops in an automated fashion. A pre-trained transformer model is then fine-tuned on the unlabeled building crops in an unsupervised manner to learn the distribution of the newly acquired data. Finally, the fine-tuned network is used to predict the damage class. Our research methodology involved in developing the proposed framework examined different data sources and deep learning architectures described in this section (Singh and Hoskere 2023).

Data Sources, Collection and Preparation

We compare the efficacy of images from two data sources: satellite images from Google Satellite Images[2] and UHRA images from Vexcel Imaging[4]. In this study, we use a 5-class scale for building damage, numbered 0 to 4, representing the severity of the damage.

Our dataset was built using multiple online resources, including DesignSafe, the Google Maps Geocoding API and Vexcel Imaging. For the labeled dataset, NEHRI's DesignSafe website was utilized to obtain building coordinates and manually inspected damage class by Kijewaski-Correa et al. (Kijewski et al. 2018). The Google Maps Geocoding API was then employed to get the building footprint as a polygon. Finally, the Vexcel imaging API was used to extract the corresponding image and associate it with its respective damage class. These images are extracted using the input of the time of the event and a building polygon. Following this procedure, 1072 labeled images and 16800 unlabeled were extracted, Figure 2 presents a sample of each class from the extracted dataset.

UHRA Image Data

The UHRA images used in this study were acquired from Vexcel Imaging[4]. The images are captured via a fleet of fixed-winged aircraft equipped with the UltraCam, a high-resolution camera system to capture up to 1.7 cm ground sample distance (GSD). UHRA images not only overcome the limitation of low-resolution satellite images (usually 30 – 50 cm GSD) but can also be quickly acquired by aircraft over large area in a short span of time.

Satellite Image Data

The satellite images dataset used in this study was adopted from (Khajwal et. al. 2023), made publicly available on DesignSafe. The dataset consists of 500 labeled images (examples in Figure 2) extracted from Google Satellite Images. There are several other satellite datasets are available as open source, as discussed in the introduction section, such as the xBD dataset (Gupta 2019). However, we decided not to utilize this data because it classifies damage states into four different classes (no damage, minor damage, major damage, and destroyed), which deviates from the proposed 5-class scale.

Deep Learning Architectures

The Vision Transformer, also known as ViT, utilizes a Transformer-based architecture to classify images (Dosovitskiy et al. 2020). It operates by dividing an image into fixed-size non-overlapping patches, followed by a linear projection of each patch. Position embeddings are then added to each patch, and the resultant sequence of

[2] https://earth.google.com

vectors is passed through a standard Transformer encoder (Dosovitskiy 2020). The Transformer encoder includes a Multi-Head Self Attention Layer, a Multi-Layer Perceptron (MLP) Layer with Gaussian Error Linear Unit. Layer Normalization is applied before each of these layers. In our study, we used a pre-trained model trained on ImageNet (Deng et al. 2010) to speed up training, improve performance, and leverage learned representations.

The Semi-Supervised Vision Transformer (Semi-ViT) (Cai et. al. 2022a) is a transformer-based model as the name suggests but utilizes unlabeled data along with labeled data. The semi-supervised learning pipeline comprises three stages: pre-training (Transfer learning (Bouchard Kalaitzis 2022)), followed by supervised fine-tuning, and eventually semi-supervised fine-tuning.

In our study, we used the same pretrained model and supervised training procedure as described in the previous section. During the semi-supervised fine-tuning phase, the exponential moving average (EMA)-Teacher framework is adopted. This choice was driven by the fact that recent results from (Cai et al. 2022) suggest that the EMA-Teacher framework provides better stability and achieves higher accuracy for semi-supervised vision transformers for classification tasks compared to the more commonly used FixMatch method. The EMA-teacher framework consists of two parallel networks, the student network and the teacher network, both of which are initialized as the fully supervised ViT model trained on labelled data.

Experiments

Examining the potency of unlabeled data, optimizing model architecture, and assessing various data types are pivotal for constructing an automated PDA framework. This study addresses three key research questions: (i) comparing CNN and Transformer architectures to pinpoint the superior predictor for damage class; (ii) gauging the impact of unlabeled data on predictive accuracy, hypothesizing its enhancement when combined with labeled data; and (iii) contrasting satellite and UHRA Image data in feature extraction and generalization. Models employ 85% of data for training and 15% for testing, summarized in Table 1. These findings bolster the refinement of accurate, resilient post-disaster damage assessment models. The ensuing sub-section outlines the experiments crafted to test our hypotheses.

Comparison of CNN and Transformer Model Architectures

We contrasted CNN and transformer models to determine the more adept architecture. A Vision Transformer (ViT) model (Sat-ViT-100) was evaluated alongside a CNN model from (Khajwal and Noshadravan 2023) (Sat-CNN-100) (Table 1), ensuring equitable data usage for fair comparison.

Semi-Supervised Learning with Unlabeled Data

We explored model performance with limited labeled data and the potential of incorporating abundant unlabeled data. Two experiments were designed: UHR-Semi-100 with 100% labeled and 100% unlabeled data, and UHR-Semi-50 with 25% labeled and 100% unlabeled data (Table 1). These cases were compared against supervised baselines (UHR-ViT-100 and UHR-ViT-25), simulating real-world scenarios where labeled data scarcity prevails.

Name	Data Source	Model Type	Train data (%)	Method
Sat-CNN-100	Satellite	CNN	100	Supervised
Sat-ViT-100	Satellite	(ViT)	100	Supervised
UHR-ViT-100	UHRA	(ViT)	100	Supervised
UHR-ViT-25	UHRA	(ViT)	25	Supervised
UHR-Semi-100	UHRA	Semi-ViT	100	SS
UHR-Semi-25	UHRA	Semi-ViT	25	SS

SS = Semi-Supervised

Table 1. Summary of experiments

Comparison of Satellite and UHRA Image Data Types

We quantitatively and qualitatively compared models trained on Satellite and Ultra-High-Resolution Aerial (UHRA) Images for damage classification. Two ViT models were trained on each data source and tested on both (Table 2).

Model Name	Trained on	Tested on
ViT-UHR-UHR	UHRA (213)	UHRA (54)
ViT-UHR-Sat	UHRA (213)	Satellite (54)
ViT-Sat-Sat	Satellite (213)	Satellite (54)
ViT-Sat-UHR	Satellite (213)	UHRA (54)

Table 2. Summary of Inter-data Experiments

Results and Discussion

This section presents findings from three experiments detailed earlier, with results summarized in Table 3, providing insights for enhancing model performance and data selection in an automated PDA framework.

Name	A	F1	P	RC	AUC
UHR-Semi-100	88	88	89	88	96
UHR-ViT-100	81	77	79	77	94
UHR-Semi-25	81	83	84	82	91
Sat-ViT-100	73	72	72	73	88
UHR-ViT-25	71	68	70	68	91
Sat-CNN-100	55	54	55	55	78

*A = Accuracy, F1 = F1 score, P = Precession, RC = Recall, AUC = Area under the ROC curve, all values in %

Table 3. Performance report for different experiments

Comparison of CNN and Transformer Model Architectures

Comparing CNN and Transformer models, the transformer-based architecture significantly outperforms the CNN-based model, exhibiting an 18% higher accuracy (Sat-CNN-100 vs. Sat-ViT-100). The transformer model's reliability and its capability to surpass human-level accuracy on satellite images substantiate its suitability for practical applications.

Model Name	Accuracy (%)	F1 (%)	Average AUC ROC (%)
ViT-UHR-Sat	58	62	83
ViT-Sat-UHR	41	39	76
ViT-UHR-UHR	71	68	91
ViT-Sat-Sat	67	66	91

Table 4. Summary of Inter-data Experiments

Semi-Supervised Learning with Unlabeled Data

Through experiments UHR-ViT-100, UHR-Semi-100, UHR-ViT-25, and UHR-Semi-25, we demonstrate the effectiveness of semi-supervised training using unlabeled data. Notably, incorporating unlabeled data yields accuracy gains of 7% and 10% for UHR-ViT-100 and UHR-ViT-25, respectively (Figure 3). These results underscore the potency of semi-supervised training to enhance model performance by leveraging additional data. Confusion matrix (Figure 4) clearly demonstrates the discriminative capabilities in distinguishing between different classes and its consistent performance across all damage states.

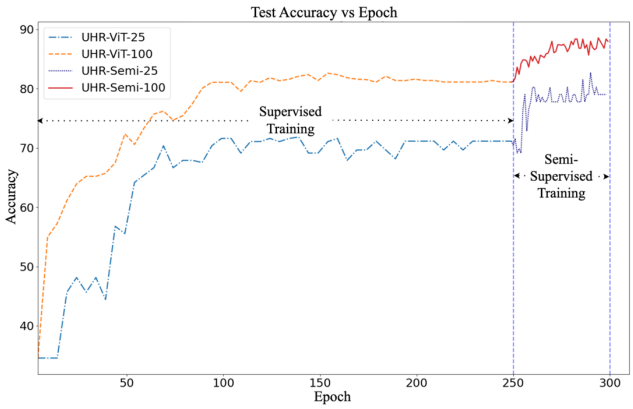

Figure 3: Learning Curve for Experiments UHR-Semi-25 and UHR-Semi-100

Comparison of Satellite and UHRA Data

Evaluating satellite and UHRA data, models trained on UHRA images exhibit better generalization capabilities. The results are all the experiments are summarized in Table 4. According to the experimental results, the model trained on UHRA images and tested on satellite images yielded the AUC-ROC of 83%, whereas the model trained on satellite images and tested on UHRA yielded 76%. The analysis of Class Activation Maps (CAMs) (Figure 5) further confirms

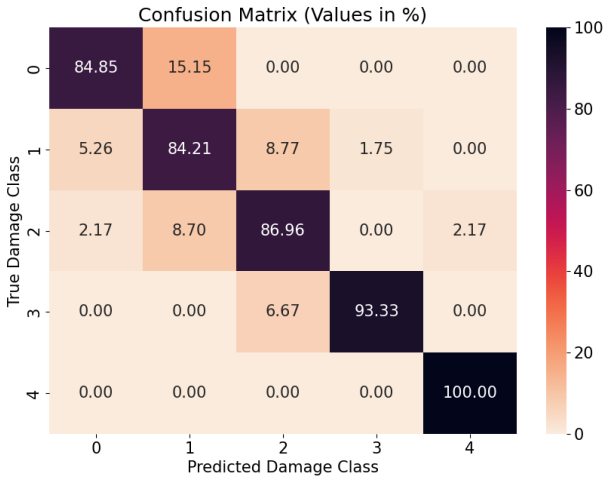

Figure 4: Confusion matrix for UHR-Semi-100

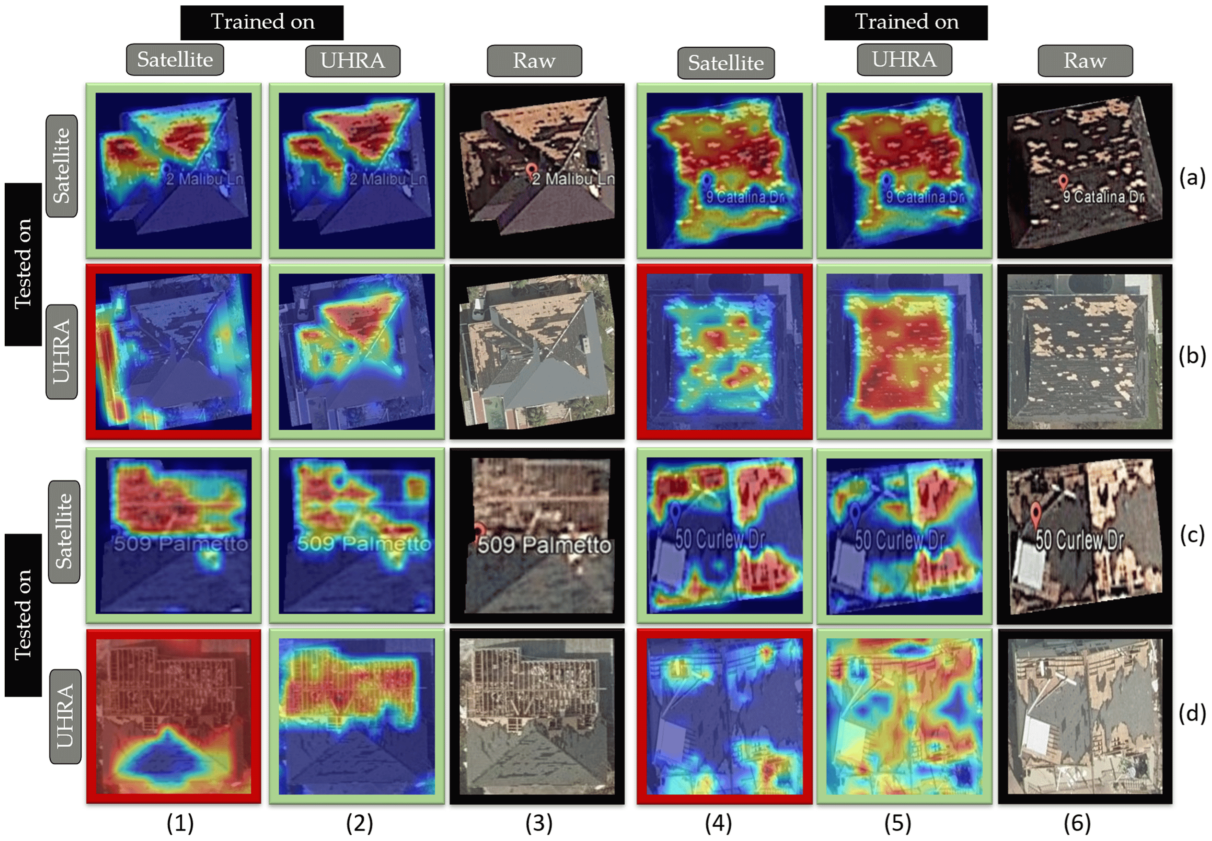

Figure 5. Class Activation Maps (CAMs) showing good CAMs in green box and bad CAMs in red.

the model's robustness in utilizing UHRA images for accurate damage assessment. These results affirm the practical significance of UHRA imagery in enhancing the framework's overall performance.

Conclusions

Developing an efficient, accurate, and automatic preliminary disaster assessment (PDA) is necessary for the speedy recovery of affected communities. Our research makes novel contributions towards such an assessment by incorporating (i) Ultra High-Resolution Aerial (UHRA) images, (ii) large amounts of unlabeled data with semi-supervised learning, and (iii) vision-transformer models. Our best model uses a semi-supervised vision transformer with UHRA data and achieved an 88% 5-class accuracy, improving over prior state-of-the-art supervised CNN model with satellite data by 33%. Notably, unlabeled data improved supervised vision transformer model accuracy by 10% for the model trained on just 213 labelled images. When comparing supervised models on satellite data as well, the vision transformer performed significantly better, producing a 73% accuracy compared to 55% using a CNN. Additionally, our experiments reveal that the inclusion of UHRA images during training not only improves the model's capacity to adapt to satellite data but also enhances the model's proficiency in distinguishing between different classes. The findings of this study will greatly expedite and enhance both post-disaster assessment and the overall recovery process and enable more climate resilient communities.

Acknowledgments

This work was conducted at the University of Houston under a contract with the Commercial Smallsat Data Scientific Analysis Program of NASA (NNH22ZDA001N-CSDSA) and the High Priority Area Research Seed Grant from the University of Houston (Grant number 000182561). The authors acknowledge the use of the Carya Cluster and the advanced support from the Research Computing Data Core at the University of Houston to carry out the research presented here. The authors would also like to acknowledge Vexcel Imaging for access to their data.

References

Abdi, G. and Jabari, S. 2021. A Multi-Feature Fusion Using Deep Transfer Learning for Earthquake Building Damage

Detection. *Canadian Journal of Remote Sensing*, 47, 337–352. doi.org/10.1080/07038992.2021.1925530.

Aicardi, I., Nex, F., Gerke, M. and Lingua, A.M. 2016. An image-based approach for the Co-registration of multi-temporal UAV image datasets. *Remote Sensing*, 8. doi.org/10.3390/RS8090779.

Asokan, A. and Anitha, J. 2019. Change detection techniques for remote sensing applications: a survey. *Earth Science Informatics*, 12, 143–160. doi.org/10.1007/S12145-019-00380-5/FIGURES/6.

Bai, Y., Hu, J., et al. 2020. Pyramid Pooling Module-Based Semi-Siamese Network: A Benchmark Model for Assessing Building Damage from xBD Satellite Imagery Datasets. *Remote Sensing 2020, Vol. 12, Page 4055*, 12, 4055. doi.org/10.3390/RS12244055.

Berezina, P. and Liu, D. 2022. Hurricane damage assessment using coupled convolutional neural networks: a case study of hurricane Michael. 13, 414–431. doi.org/10.1080/19475705.2022.2030414.

Bouchard, I., Rancourt, M.È., Aloise, D. and Kalaitzis, F. 2022. On Transfer Learning for Building Damage Assessment from Satellite Imagery in Emergency Contexts. *Remote Sensing 2022, Vol. 14, Page 2532*, 14, 2532. doi.org/10.3390/RS14112532.

Cai, Z., Ravichandran, A., et al. 2022. Semi-supervised Vision Transformers at Scale. *arXiv*, arXiv:2208.05688. doi.org/10.48550/ARXIV.2208.05688.

Calantropio, A., Chiabrando, F., Codastefano, M. and Bourke, E. 2021. Deep learning for automatic building damage assessment: application in post-disaster scenarios using UAV data. *ISPRS Annals of the Photogrammetry, Remote Sensing and Spatial Information Sciences*, 5, 113–120. doi.org/10.5194/ISPRS-ANNALS-V-1-2021-113-2021.

Celik, T. 2009. Unsupervised change detection in satellite images using principal component analysis and κ-means clustering. *IEEE Geoscience and Remote Sensing Letters*, 6, 772–776. doi.org/10.1109/LGRS.2009.2025059.

Celik, T. 2010. Change detection in satellite images using a genetic algorithm approach. *IEEE Geoscience and Remote Sensing Letters*, 7, 386–390. doi.org/10.1109/LGRS.2009.2037024.

Chen, J., Yuan, Z., et al. 2021. DASNet: Dual Attentive Fully Convolutional Siamese Networks for Change Detection in High-Resolution Satellite Images. *IEEE Journal of Selected Topics in Applied Earth Observations and Remote Sensing*, 14, 1194–1206. doi.org/10.1109/JSTARS.2020.3037893.

Deng, J., Dong, W., Socher, R., Li, L.-J., Kai Li and Li Fei-Fei. 2010. ImageNet: A large-scale hierarchical image database. *IEEE conference on computer vision and pattern recognition.*, 248–255. doi.org/10.1109/CVPR.2009.5206848.

Dosovitskiy, A., Beyer, L., et al. 2020. An Image is Worth 16x16 Words: Transformers for Image Recognition at Scale. *ICLR 2021 - 9th International Conference on Learning Representations*.

Ezequiel, C.A.F., Cua, M., et al. 2014. UAV aerial imaging applications for post-disaster assessment, environmental management and infrastructure development. *2014 International Conference on Unmanned Aircraft Systems, ICUAS 2014 - Conference Proceedings*, 274–283. doi.org/10.1109/ICUAS.2014.6842266.

Gupta, R., Hosfelt, R., et al. 2019b. xBD: A Dataset for Assessing Building Damage from Satellite Imagery. *IEEE Computer Society Conference on Computer Vision and Pattern Recognition Workshops*, 10–17.

Hong, Z., Zhong, H., et al. 2022. Classification of Building Damage Using a Novel Convolutional Neural Network Based on Post-Disaster Aerial Images. *Sensors 2022, Vol. 22, Page 5920*, 22, 5920. doi.org/10.3390/S22155920.

Hoskere, V., Narazaki, Y., et al. 2018. Towards Automated Post-Earthquake Inspections with Deep Learning-based Condition-Aware Models. *arXiv*, arXiv:1809.09195. doi.org/10.48550/ARXIV.1809.09195.

Irish, J.L., Sleath, A., Cialone, M.A., Knutson, T.R. and Jensen, R.E. 2014. Simulations of Hurricane Katrina (2005) under sea level and climate conditions for 1900. *Climatic Change*, 122, 635–649. doi.org/10.1007/S10584-013-1011-1.

Khajwal, A.B., Cheng, C.S. and Noshadravan, A. 2023. Post-disaster damage classification based on deep multi-view image fusion. *Computer-Aided Civil and Infrastructure Engineering*, 38, 528–544. doi.org/10.1111/MICE.12890.

Kijewski-Correa, T., gong, jie, et al. 2018. Hurricane Harvey (Texas) Supplement -- Collaborative Research: Geotechnical Extreme Events Reconnaissance (GEER) Association: Turning Disaster into Knowledge. doi.org/10.17603/DS2Q38J.

Kim, M., Park, S.E. and Lee, S.J. 2023. Detection of Damaged Buildings Using Temporal SAR Data with Different Observation Modes. *Remote Sensing 2023, Vol. 15, Page 308*, 15, 308. doi.org/10.3390/RS15020308.

Lee, J., Xu, J.Z., et al. 2020. Assessing Post-Disaster Damage from Satellite Imagery using Semi-Supervised Learning Techniques. *arXiv*, arXiv:2011.14004. doi.org/10.48550/ARXIV.2011.14004.

Lu, C.H., Ni, C.F., Chang, C.P., Yen, J.Y. and Chuang, R.Y. 2018. Coherence difference analysis of sentinel-1 SAR interferogram to identify earthquake-induced disasters in urban areas. *Remote Sensing*, 10. doi.org/10.3390/RS10081318.

Matsuoka, M. and Yamazaki, F. 2004. Use of satellite SAR intensity imagery for detecting building areas damaged due to earthquakes. *Earthquake Spectra*, 20, 975–994. doi.org/10.1193/1.1774182.

Matsuoka, M. and Yamazaki, F. 2005. Building damage mapping of the 2003 Bam, Iran, earthquake using Envisat/ASAR intensity imagery. *Earthquake Spectra*, 21. doi.org/10.1193/1.2101027.

Mavroulis, S., Andreadakis, E., et al. 2019. UAV and GIS based rapid earthquake-induced building damage assessment and methodology for EMS-98 isoseismal map drawing: The June 12, 2017 Mw 6.3 Lesvos (Northeastern Aegean, Greece) earthquake. *International Journal of Disaster Risk Reduction*, 37, 101169. doi.org/10.1016/J.IJDRR.2019.101169.

Narazaki, Y., Hoskere, V., Chowdhary, G. and Spencer, B.F. 2022. Vision-based navigation planning for autono-

mous post-earthquake inspection of reinforced concrete railway viaducts using unmanned aerial vehicles. *Automation in Construction*, 137, 104214. doi.org/10.1016/J.AUTCON.2022.104214.

Rahnemoonfar, M., Chowdhury, T., Murphy, R., Rahnemoonfar, M., Chowdhury, T. and Murphy, R. 2022. RescueNet: A High Resolution UAV Semantic Segmentation Benchmark Dataset for Natural Disaster Damage Assessment. *arXiv*, arXiv:2202.12361. doi.org/10.48550/ARXIV.2202.12361.

Reese, S. 2018. FEMA Individual Assistance Programs: In Brief. *Congressional Research Service, Washington DC*.

Singh, D.K. and Hoskere, V. 2023. Post Disaster Damage Assessment Using Ultra-High-Resolution Aerial Imagery with Semi-Supervised Transformers. *Sensors 2023, Vol. 23, Page 8235*, 23, 8235. doi.org/10.3390/S23198235.

Watanabe, M., Thapa, R.B., Ohsumi, T., Fujiwara, H., Yonezawa, C., Tomii, N. and Suzuki, S. 2016. Detection of damaged urban areas using interferometric SAR coherence change with PALSAR-2 4. Seismology. *Earth, Planets and Space*, 68. doi.org/10.1186/S40623-016-0513-2.

Woodward, A.J. and Samet, J.M. 2018. Climate Change, Hurricanes, and Health. *American Journal of Public Health*, 108, 33. doi.org/10.2105/AJPH.2017.304197.